Diffusion barriers block defect occupation on reduced CeO_2(111)

P. G. Lustemberg*
Instituto de Física Rosario (IFIR, CONICET-UNR) and Facultad de Ciencias Exactas, Ingeniería y Agrimensura (UNR), 2000 Rosario, Argentina

Yi Pan*
Institute of Physics, Chinese Academy of Sciences, P.O. Box 603, Beijing 100190, China

B. -J. Shaw, D. Grinter, Chi Pang, and G. Thornton
Department of Chemistry and London Centre for Nanotechnology, University College London, London WC1H 0AJ, United Kingdom

R. Pérez
Departamento de Física Teórica de la Materia Condensada and Condensed Matter Physics Center (IFIMAC), Universidad Autonoma de Madrid, 28049 Madrid, Spain

M. V. Ganduglia-Pirovano†
Instituto de Catálisis y Petroleoquímica (ICP-CSIC), 28049 Madrid, Spain

N. Nilius‡
Institute of Physics, Carl von Ossietzky University, 26111 Oldenburg, Germany
(Dated: April 25, 2016)

Figure S1 shows the clean and defective ceria (111) surfaces with the atom color scheme used in this work.

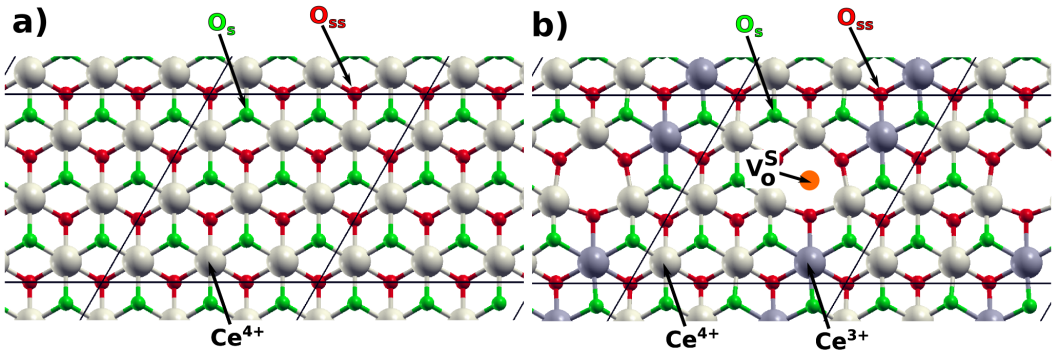

FIG. S1: a) Clean CeO_2 (111) surface and b) defective CeO_{2-x} (111) surface with one surface oxygen vacancy (V_o^s). The Ce^{4+} and Ce^{3+} ions and the surface and subsurface O atoms are depicted in white, gray, green and red, respectively.

A. Au Atom Adsorption

Tables S1 and S2 show the calculated Au adsorption energy and its charge state, using the PBE+U approach and the HSE06 functional, for Au on various positions, and for different configurations of the Ce^{3+} ions. In all the cases, a $2 \times 2 \times 1$ k-point mesh has been employed. With PBE+U, two cases have been considered: *i*) optimization of the Au atom coordinates, keeping the initially relaxed surfaces *frozen*, and *ii*) full geometry optimization, including Au and the atoms of the outermost oxide trilayer. With HSE, only full optimization has been carried out. The corresponding structures are shown in Figs. S2 and S3.

---

* both authors contributed equally to this work
†Electronic address: vpg@icp.csic.es
‡Electronic address: niklas.nilius@uni-oldenburg.de

TABLE S1: PBE+U and HSE06 adsorption energies (in eV) for one gold atom on the clean CeO_2 (111) surface. Also, the number of Ce^{3+} ions and the Au oxidation state are shown. The symbol * denotes unstable states.

Adsorption Site	PBE+U						HSE06		
	Frozen Surface[a]			1° Trilayer Relaxed			1° Trilayer Relaxed		
	No. Ce^{3+}	Au State	E_{ads} (eV)	No. Ce^{3+}	Au State	E_{ads} (eV)	No. Ce^{3+}	Au State	E_{ads} (eV)
O-bridge.a	0	Au^0	−0.72	1	Au^{1+}	−1.05	1	Au^{1+}	−0.42
O-bridge.b	0	Au^0	−0.72	1	Au^{1+}	−0.97	–	–	–
O-bridge.c	0	Au^0	−0.72	1	Au^{1+}	−0.88	–	–	–
O-hollow	0	Au^0	−0.60	1	Au^{1+}	−0.90	1	Au^{1+}	−0.29
O-top.a	0	Au^0	−0.68	1	Au^{1+}	−0.87	1	Au^{1+}	−0.35
O-top.b	0	Au^0	−0.68	1	Au^{1+}	−0.84	1	Au^{1+}	−0.35
O-top.c	0	Au^0	−0.68	1	Au^{1+}	−0.98	–	–	–
O-top.d	0	Au^0	−0.68	1	Au^{1+}	−0.98	–	–	–
Ce-top.a	–	–	–	0	Au^0	−0.40	–	–	–
Ce-top.b	–	–	–	0	Au^0	−0.40	–	–	–
OCe-bridge.a	0	Au^0	−0.65	1	Au^{1+}	−0.80	–	–	–
OCe-bridge.b	–	–	–	1	Au^{1+}	−0.95	–	–	–
Ce-bridge	0	Au^0	−0.72	1	Au^{1+}	−0.80	–	–	–
O-dhollow	*	*	*	*	*	*	–	–	–

[a]The 1° trilayer was optimized before Au adsorption

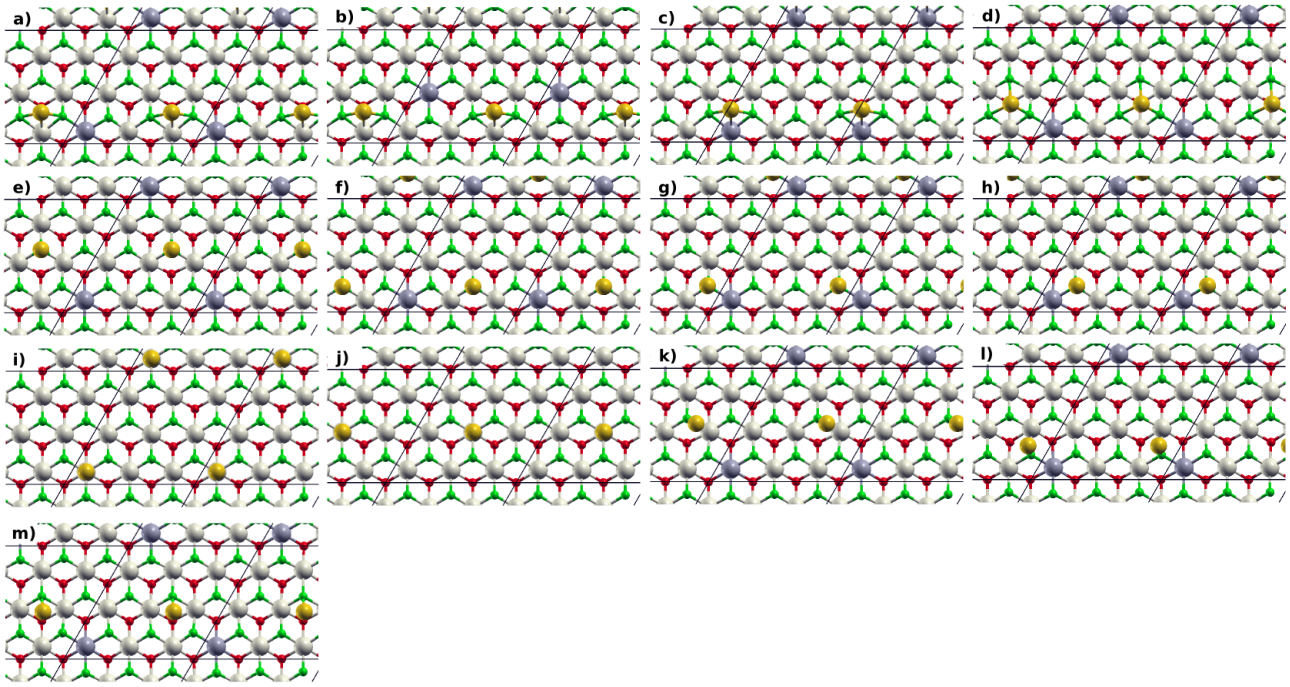

FIG. S2: Au adsorption configurations on CeO_2(111): a) O-bridge.a, b) O-bridge.b, c) O-bridge.c, d) O-hollow, e) O-top.a, f) O-top.b, g) O-top.c, h) O-top.d, i) Ce-top.a, j) Ce-top.b, k) OCe-bridge.a, l) OCe-bridge.b, and and m) Ce-bridge.

TABLE S2: PBE+U and HSE06 adsorption energies (in eV) for one gold atom on CeO_{2-x} (111) with one surface oxygen vacancy. Also, the number of Ce^{3+} ions and the Au oxidation state are shown. The symbol * denotes unstable states.

Adsorption Site	PBE+U						HSE06		
	Frozen Surface[a]			1° Trilayer Relaxed			1° Trilayer Relaxed		
	No. Ce^{3+}	Au State	E_{ads} (eV)	No. Ce^{3+}	Au State	E_{ads} (eV)	No. Ce^{3+}	Au State	E_{ads} (eV)
Ov-hollow.a	2	Au^0	−1.39	1	Au^{1-}	−2.37	1	Au^{1-}	−2.39
Ov-hollow.b	2	Au^0	−1.39	1	Au^{1-}	−2.29	–	–	–
Ov-hollow.c	2	Au^0	−1.39	1	Au^{1-}	−2.22	–	–	–
O-top.a	*	*	*	3	Au^{1+}	−0.97	3	Au^{1+}	−0.42
O-top.b	2	Au^0	−0.66	3	Au^{1+}	−0.89	–	–	–
O-top.c	*	*	*	3	Au^{1+}	−0.86	–	–	–
O-top.d	*	*	*	2	Au^0	−0.71	–	–	–
O-top.e	*	*	*	3	Au^{1+}	−0.70	–	–	–
O-top.f	*	*	*	3	Au^{1+}	−0.85	–	–	–
O-dhollow.a	2	Au^0	−0.90	2	Au^0	−1.06	2	Au^0	−0.80
O-dhollow.b	2	Au^0	−0.90	2	Au^0	−1.05	2	Au^0	−0.81
O-dhollow.c	2	Au^0	−0.89	2	Au^0	−0.95	–	–	–
O-dhollow.d	–	–	–	2	Au^0	−1.01	–	–	–
O-hollow	*	*	*	2	Au^0	−0.93	2	Au^0	−0.58
Ce-bridge	2	Au^0	−0.68	3	Au^{1+}	−0.87	–	–	–
O-bridge.a	2	Au^0	−0.68	3	Au^{1+}	−1.00	3	Au^{1+}	−0.32
O-bridge.b	*	*	*	3	Au^{1+}	−1.00	–	–	–
O-bridge.c	2	Au^0	−0.51	3	Au^{1+}	−0.95	–	–	–
O-bridge.d	*	*	*	3	Au^{1+}	−0.90	3	Au^{1+}	−0.20
O-bridge.e	2	Au^0	−0.67	3	Au^{1+}	−0.85	–	–	–
O-bridge.f	2	Au^0	−0.68	3	Au^{1+}	−0.83	–	–	–
O-bridge.g	*	*	*	3	Au^{1+}	−0.82	3	Au^{1+}	−0.11
O-bridge.h	*	*	*	3	Au^{1+}	−0.85	3	Au^{1+}	−0.11

[a]The 1° trilayer was optimized before Au adsorption

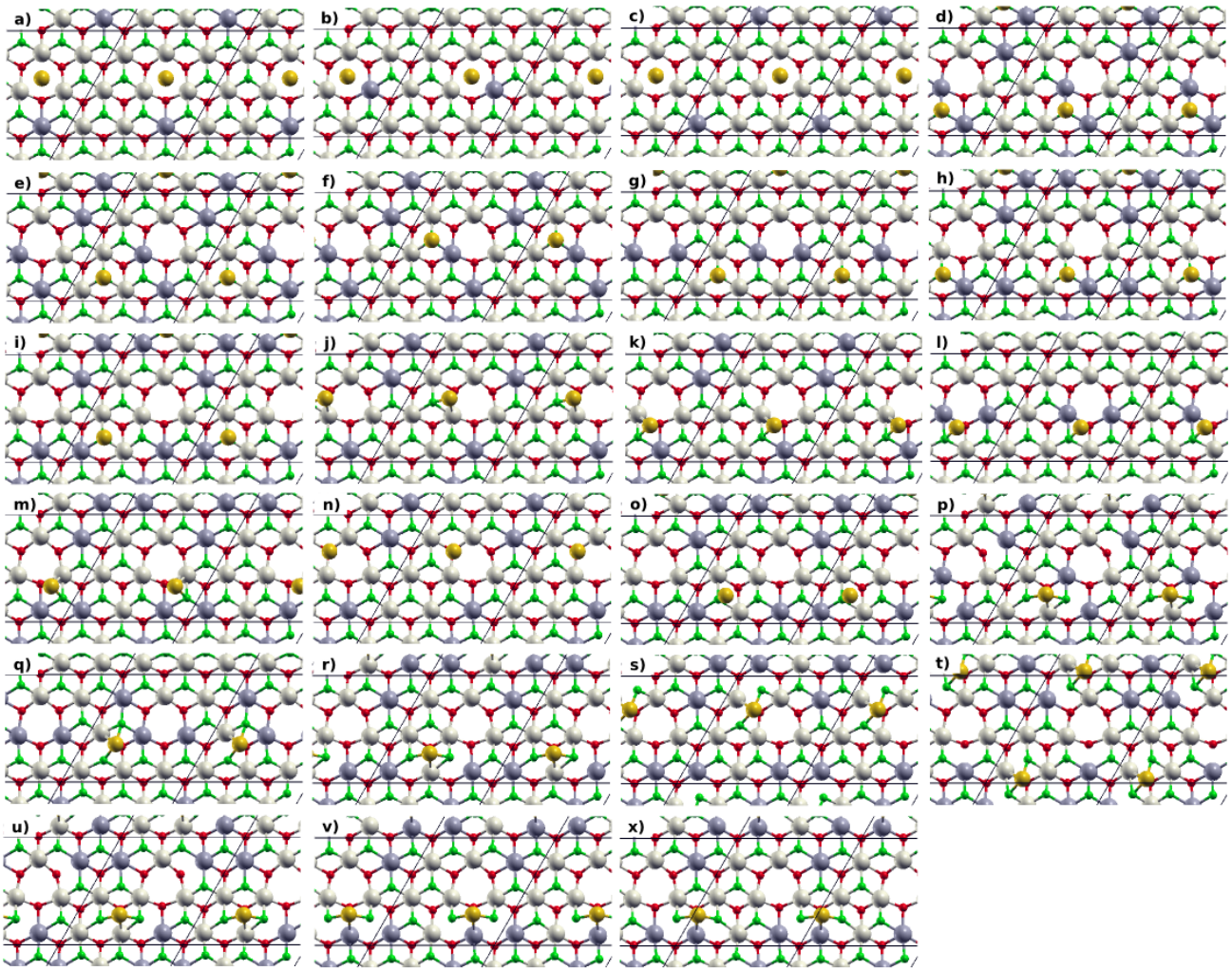

FIG. S3: Au adsorption configurations on $CeO_{2-x}(111)$ with one surface oxygen vacancy: a) V_o^s-hollow.a, b) V_o^s-hollow.b, c) V_o^s-hollow.c, d) O-top.a, e) O-top.b, f) O-top.c, g) O-top.d, h) O-top.f, i) O-dhollow.a, j) O-dhollow.b, k) O-dhollow.c, l) O-dhollow.d, m) O-hollow, o) Ce-bridge, p) O-bridge.a, q) O-bridge.b, r) O-bridge.c, s) O-bridge.d, t) O-bridge.e, u) O-bridge.f, v) O-bridge.g, and x) O-bridge.h.

B. Au Diffusion Pathways

1. *Clean CeO_2(111) Surface*

The Au diffusion pathways on the clean $CeO_2(111)$ surface are shown in Fig. S4. Two scenarios were considered, namely, adiabatic (red energy profile in the lower panel) and diabatic diffusion. For the adiabatic case, relaxations include the Au atom and the atoms of the outermost oxide trilayer. For the diabatic case, the ceria lattice and the Au charge state were kept *frozen* along the path, and two configurations were considered: *i*) diffusion on the pristine (relaxed) ceria surface (upper panel), and *ii*) diffusion on a surface that corresponds to the relaxed structure for Au adsorption on a particular site (blue, green, yellow, and magenta energy profiles in the lower panel).

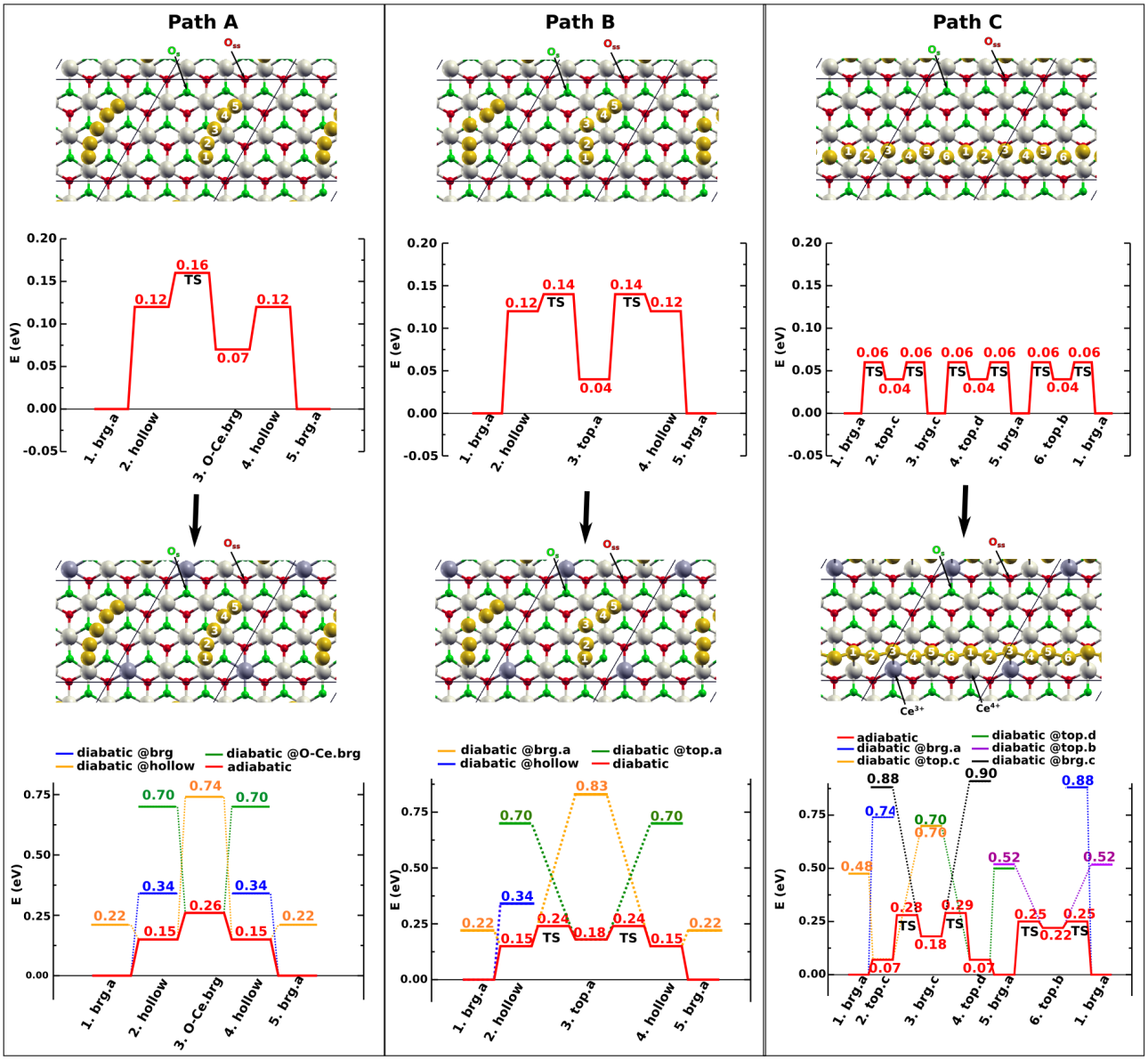

FIG. S4: Diffusion pathways for Au on $CeO_2(111)$: diabatic (upper panel) on the frozen pristine (relaxed) ceria surface, adiabatic (lower panel, red profile), and diabatic (lower panel, blue, green, yellow, and magenta profiles) on a frozen surface that corresponds to the relaxed structure for a particular Au adsorption site.

TABLE S3: Values of the imaginary frequency vibration of the transition states along the Diabatic and Adiabatic diffusion pathways shown in the upper and lower panel, respectively, of Fig. S4.

Clean Surface		
Reaction Pathway	Diabatic (Unrelax Surf.)	Adiabatic
path.A	40 cm^{-1}	–
path.B	39 cm^{-1}	43 cm^{-1}
	39 cm^{-1}	43 cm^{-1}
path.C	38 cm^{-1}	49 cm^{-1}
	38 cm^{-1}	51 cm^{-1}
	38 cm^{-1}	46 cm^{-1}
	38 cm^{-1}	46 cm^{-1}

2. *Defective CeO_{2-x}(111) Surface*

For the defective surface, adiabatic and diabatic diffusion pathways were considered. Figure S5 shows the diabatic path for Au diffusion on the frozen defective surface with an oxygen vacancy. Here, surface atoms were not optimized as the Au atom moved. For this reason, the oxidation state of Au is zero along the path. This path shows two transition states with energies of 0.06 and -0.16 eV that are characterized by having the same imaginary frequency of 40 cm^{-1}.

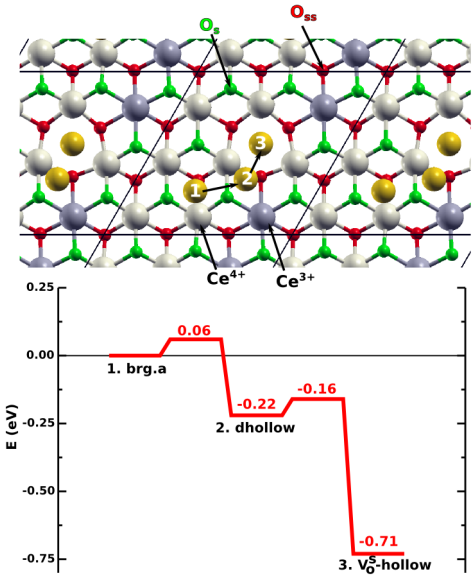

FIG. S5: Diabatic diffusion pathway for Au on the frozen (relaxed) ceria surface with one V_o^s.

Figure S6 shows energy profiles for five adiabatic diffusion pathways (red), and various diabatic pathways on surfaces that correspond to relaxed structures for Au adsorption on a particular site (blue, green, yellow, and magenta energy profiles). Path.A has a transition state (TS) with an energy of 0.23 eV and imaginary frequency of 46 cm^{-1} and for Path.B these values are 0.22 eV and 46 cm^{-1}, respectively. Path.C has two TS with an energy of 0.16 eV and 0.10 eV and imaginary frequencies of 50 cm^{-1} and 41 cm^{-1}, respectively. Path.D has a TS with an energy equal 0.31 eV and an imaginary frequency of 42 cm^{-1}. Finally, Path.E has six transition states with energies: 0.22, 0.12, 0.10, 0.00, 0.15 and 0.21 eV, characterized by an imaginary frequency of 47, 44, 42, 40, 45 and 46 cm^{-1}, respectively.

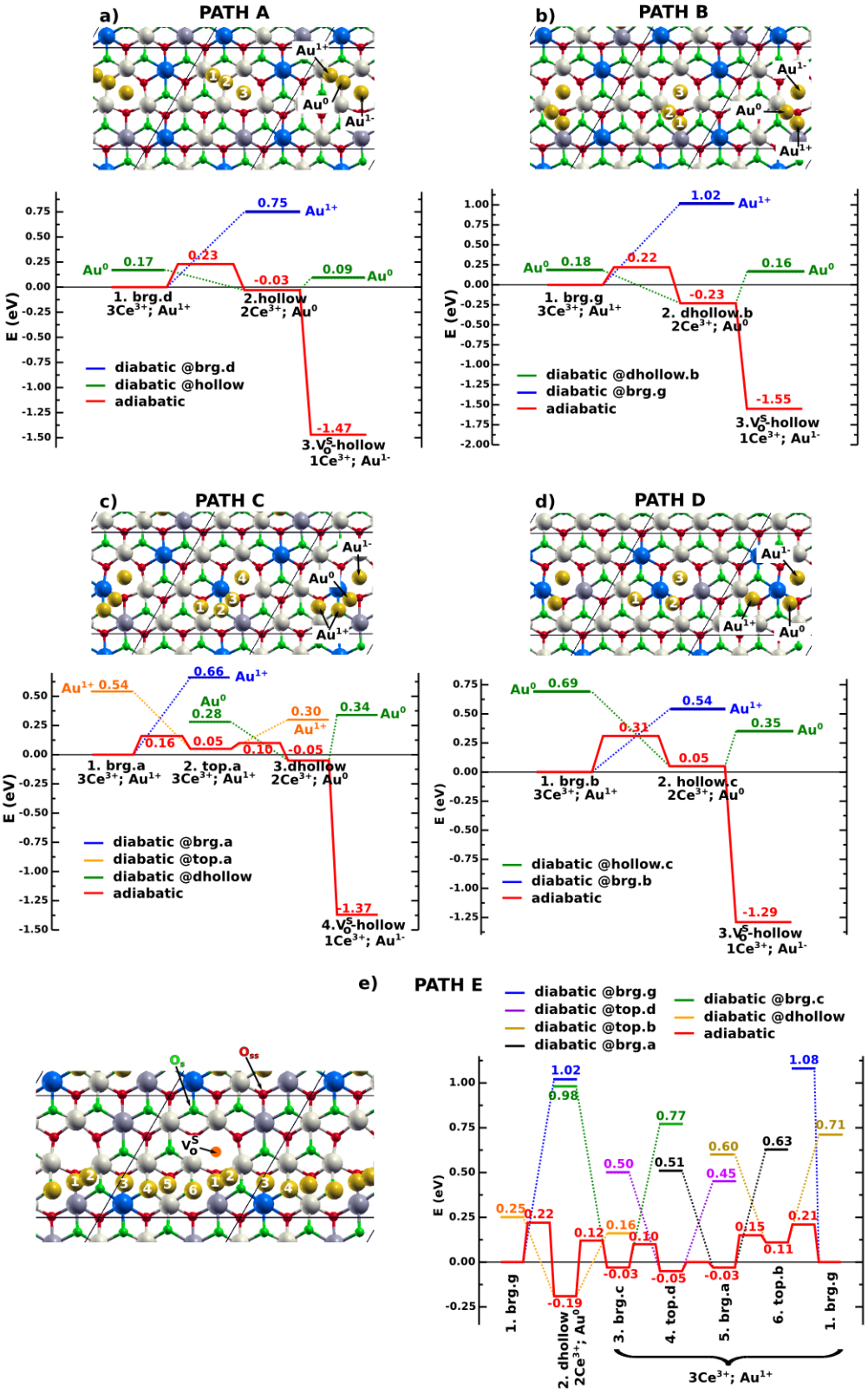

FIG. S6: Adiabatic and diabatic Au diffusion pathways on the defective $CeO_{2-x}(111)$ surface with one oxygen vacancy, V_o^s.

TABLE S4: Values of the imaginary frequency vibration of the transition states along the adiabatic diffusion pathways shown in Fig. S6.

Defective Surface	
Reaction Pathway	Adiabatic
path.A	46 cm^{-1}
path.B	46 cm^{-1}
path.C	50 cm^{-1}
	41 cm^{-1}
path.D	42 cm^{-1}
path.D	42 cm^{-1}
	44 cm^{-1}
	47 cm^{-1}
	46 cm^{-1}
	45 cm^{-1}
	43 cm^{-1}